

## Article

# Predicting Sub-Forest Type Transition Characteristics Using Canopy Density: An Analysis of the Ganjiang River Basin Case Study

Yuchen Zhou <sup>1</sup>, Juhua Hu <sup>2</sup>, Mu Liu <sup>1,\*</sup> and Guanhong Xie <sup>1</sup><sup>1</sup> College of Forestry, Jiangxi Agricultural University, Nanchang 330045, China<sup>2</sup> College of Computer and Information Engineering, Jiangxi Agricultural University, Nanchang 330045, China

\* Correspondence: liumu0312@jxau.edu.cn

**Abstract:** In the process of societal development, forest land categories often conflict with other land use types, leading to impacts on the ecological environment. Therefore, research on changes in forest land categories has increasingly become a globally focused topic. To anticipate potential forest ecological security issues under urbanization trends, studies on regional land use simulation become more important. This paper, based on land use data from the Ganjiang River basin, analyzes the distribution characteristics and changing trends of land use types from 2000 to 2020. Using the CA-Markov model, it predicts the land use pattern of the basin in 2040 and analyzes the transfer characteristics of forest land categories. The conclusions indicate that, between 2000 and 2020, the most significant trend in land use evolution was the transfer between various subcategories of forest land, especially frequent in the high-altitude mountainous areas in the southern and western parts of the basin. The land use pattern prediction model constructed in this paper has a kappa index of 0.92, indicating high accuracy and reliability of the predictions. In 2040, the most significant land evolution phenomenon would be from forest land to arable land to construction land, particularly pronounced around large cities. Over the next 20 years, the focus of land use evolution may shift from the southern part of the basin to the central and northern parts, with urban expansion possibly becoming the main driving force of land use changes during this period. Forest land restoration work is an effective method to compensate for the loss of forest land area in the Ganjiang River basin, with key areas for such work including Longnan, Yudu, Xingguo, Ningdu, Lianhua, and Yongxin counties.

**Keywords:** forest land; CA-Markov model; LULC; Ganjiang River basin; land use transition

**Citation:** Zhou, Y.; Hu, J.; Liu, M.; Xie, G. Predicting Sub-Forest Type Transition Characteristics Using Canopy Density: An Analysis of the Ganjiang River Basin Case Study. *Forests* **2024**, *15*, 274. <https://doi.org/10.3390/f15020274>

Academic Editors: Jia Wang, Weiheng Xu, Jincheng Liu, Zhichao Wang, Stelian Alexandru Borz and Cate Macinnis-Ng

Received: 17 November 2023

Revised: 19 January 2024

Accepted: 27 January 2024

Published: 31 January 2024



**Copyright:** © 2024 by the authors. Licensee MDPI, Basel, Switzerland. This article is an open access article distributed under the terms and conditions of the Creative Commons Attribution (CC BY) license (<https://creativecommons.org/licenses/by/4.0/>).

## 1. Introduction

Global terrestrial ecosystems have undergone significant changes due to prolonged human social activities [1]. In recent decades, changes in Land Use and Land Cover (LULC) have intensified, with urban development and forest resource exploitation being key drivers of this phenomenon [2–4]. The National Bureau of Statistics report states that from 1982 to 2022, China’s urbanization rate increased from 20.17% to 63.89% [5]. Rapid urbanization, accompanied by high-intensity land use and rapid loss of forest land types, has increased the vulnerability of the natural environment, thereby inducing ecological crises and natural disasters, seriously threatening the sustainable development of the region [6]. To maximize the efficiency of land use policies and planning, it is necessary to reasonably predict changes in land use and simulate future land use patterns. Monitoring, evaluating, and predicting the evolution of land use, as well as studying the resulting changes in the ecological environment, will help improve the quality of urban ecological environments and human habitats [7,8]. These tasks are of great practical significance for maintaining regional sustainable development [9,10].

The Cellular Automata (CA) model was first proposed by the Hungarian-American mathematician John von Neumann in 1951, originally for simulating self-replicating behavior in cells. It is a grid-based dynamical model with discrete time, space, and states, capable of simulating the spatiotemporal evolution of complex systems. It is currently widely used in various fields such as population expansion, land use, land use assessment, and urban expansion [11–15]. The CA model also forms the basis for many composite models, such as the CLUE-S model [16,17], ANN-CA model [18,19], and Logistic-CA model [20,21]. The CA-Markov model is a more mature simulation approach, combining the CA model's capability to simulate spatial changes in complex systems with the predictive advantages of the Markov model over time, effectively overcoming the limitations of single landscape-type dynamic simulation models [22,23].

The Ganjiang River is an important river in the middle and lower reaches of the Yangtze River area, with a basin area exceeding 80,000 km<sup>2</sup>. It encompasses the most significant cities of Jiangxi Province, including Nanchang, Ji'an, and Ganzhou. These major cities are currently actively expanding their urban areas. For instance, Nanchang has increased its built-up area by 40% in the last decade, posing a significant challenge to maintaining the ecosystem service functions around the city. River basins often contain complete ecosystems, covering various topographic conditions and biological communities. Studying river basins can lead to a better understanding of the impact of land use changes on different land units and facilitate the analysis of regional ecological processes. Currently, there are no studies analyzing the characteristics of land use changes in the Ganjiang River basin or predicting land use patterns. This research aims to analyze the characteristics of land use changes in the Ganjiang River basin from 2000 to 2020, summarize the evolutionary patterns of forests with different closure degrees, and provide data references for forest ecological protection within the basin and urban planning in various cities.

## 2. Materials and Methods

### 2.1. Overview of the Study Area

The Ganjiang River, the largest river in Jiangxi Province and a major tributary of the Yangtze River, flows through a diverse landscape. The geomorphological types within the Ganjiang River basin primarily consist of mountains, hills, low mountains, plains, and water bodies. In this varied terrain, mountains and hills constitute 64.7% of the total basin area, low mountains cover 31.5%, while plains and water bodies make up only 3.9%. The basin is distinguished by its subtropical humid monsoon climate, characterized by abundant rainfall, predominantly in the spring and summer seasons [24,25]. The annual average precipitation ranges between 1400 and 1600 mm, and the average temperature hovers around 18 °C [26]. In this study, the scope of the Ganjiang River basin was established through an analysis based on the digital elevation model. We utilized the hydrologic analysis tool in ArcGIS software version 10.6 to conduct an in-depth analysis and generate shapefile format vector files. These files represent small watersheds, each delineated by ridgelines. The final determination of the basin's scope took into account the spatial relationship between the main stream of the Ganjiang River and these small watersheds. This process was further refined by integrating the county-level administrative boundaries of Jiangxi Province [27]. The resulting delineation of the Ganjiang River basin is illustrated in Figure 1.

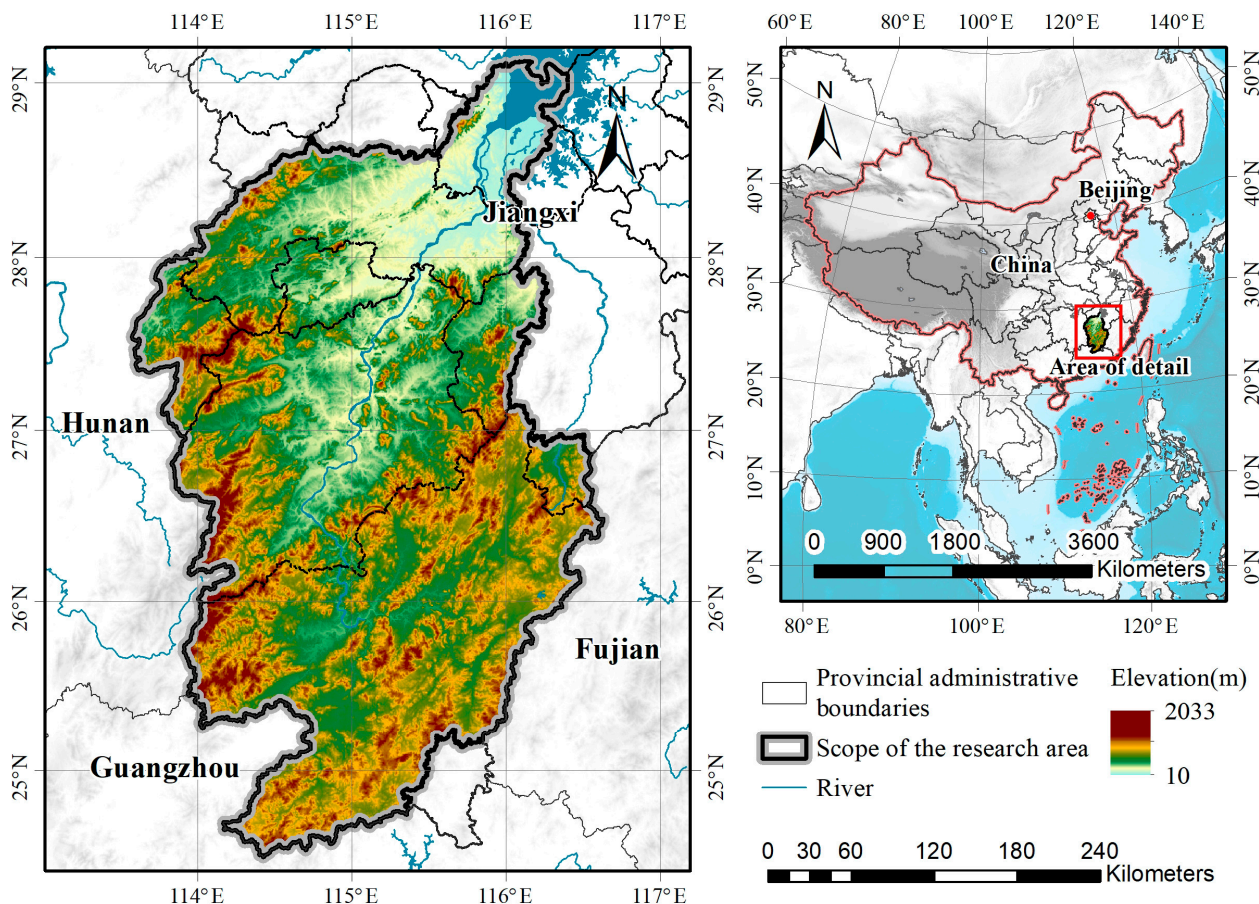


**Figure 1.** Location of the Ganjiang River basin.

## 2.2. Data Collection and Source

The data used in this paper mainly fall into four categories: land use data of the Ganjiang River basin (covering five periods, namely 2000, 2005, 2010, 2015, and 2020), the digital ground elevation model (raster data with a resolution of 30 m), meteorological data (including coordinates of meteorological stations, temperature, rainfall, and solar radiation, categorized into four types and compiled monthly from 2000 to 2020), and road distribution data (including nine types of roads). The sources of the data are listed in Table 1. Since the meteorological data are not readily available as raster data, it is necessary to use the Ordinary Kriging interpolation method during the research process to spatially interpolate and determine the meteorological changes in different areas of the study region [28,29].

**Table 1.** Data sources.

Data Name	Time	Data Source
Land use data	2000–2020	<a href="https://www.casdc.cn/">https://www.casdc.cn/</a>
Digital elevation model	/	<a href="https://earthexplorer.usgs.gov/">https://earthexplorer.usgs.gov/</a>
Meteorological station data	2000–2020	<a href="https://data.cma.cn/Market/index.html">https://data.cma.cn/Market/index.html</a>
Road distribution data	2020	<a href="https://www.resdc.cn/">https://www.resdc.cn/</a>

## 2.3. Classification of Land Use Types

This study is based on five phases of land use data from the years 2000, 2005, 2010, 2015, and 2020. Due to the high proportion of forested areas in the Ganjiang River basin and the strong spatial heterogeneity of the terrain, the characteristics of forests vary significantly across different regions. Based on the aforementioned forest characteristics and starting from the perspective of vegetation canopy density, this study divides the forest

land category into three subcategories using existing data on forest land, garden land, and grassland. These are named forest land a, forest land b, and forest land c. Forest land a represents land categories with good vegetation conditions and high ecological environmental value, encompassing secondary land types such as forested land and shrub land with a canopy density greater than 30% in the primary classification of forest land. Forest land b represents land types with lower vegetation canopy density than forest land a but still possessing certain ecological value, mainly composed of sparse forest land with a canopy density of 10%–30%. The composition of forest land c is quite unique, primarily consisting of non-cultivated vegetation-covered areas, made up of three parts. The first part includes secondary land types under the forest land category with a canopy density of less than 10%, such as unafforested land and traces of land. The second part consists of garden land, which is included due to the frequent renewal of garden plants and limited ecological value. The third part consists of grassland. Since grassland occupies a very low proportion in the study area, has limited land type changes, and mainly exists in the form of sparse forest grassland in high-altitude areas, it is also included in the category of forest land c. Together with the existing classifications of farmland, water bodies, developed land, and unused land, a total of seven land use cover categories are identified as the subjects of this study.

#### 2.4. Markov Model

The Markov model is a statistical and predictive model that can forecast a series of geographically based events characterized by their lack of subsequent effects, by calculating the probability of their occurrence.

The dynamic evolution of land use type attributes is a transformation process with Markovian properties. Assuming  $t$  is a moment in time for a particular plot in the study area, then its landscape type state at  $t + 1$  is related to its state at the time [30,31]. This process can be expressed through the following formulas:

$$S_{(t+1)} = P_{ij} \times S_t \quad (1)$$

$$P_{ij} = \frac{A_{ij}}{\sum_{j=1}^n A_{ij}} \quad (2)$$

In the above formulas,  $S$  represents the column vectors of the land use type states of the target plot at times  $t$  and  $t + 1$ ;  $P_{ij}$  represents the probability of land use type  $i$  transforming into land use type  $j$ ; and  $A_{ij}$  represents the area of the study region in which land use type  $i$  transforms into land use type  $j$ .

After establishing the transition probability of the attributes of the land use type elements, a transition matrix is constructed, as follows:

$$P_{ij} = \begin{bmatrix} P_{11} & \cdots & P_{1n} \\ \vdots & & \vdots \\ P_{n1} & \cdots & P_{nn} \end{bmatrix} \quad (3)$$

In the above formula,  $P_{ij}$  represents the probability of land use type  $i$  changing to  $j$  and  $1 \geq P_{ij} \geq 0$ , with  $\sum_{j=1}^n P_{ij} = 1$ , meaning the sum of each row's elements in the matrix equals 1.

In this study, this step is implemented using IDRISI software version 17.0. By inputting land use data from two different time points into the Markov tool, the software generates data on the potential conversion areas for each land use type at these two time points, as well as predicted values for the area of each land use type.

### 2.5. Analysis of the Correlation between Environmental Factors and Land Use Types and Selection of Research Scale

To study the impact of various environmental factors on land use types, we need to have an overall understanding of the correlation between the two sets of data [32,33]. Before this, we need to choose the spatial scale for the correlation study. Scale effect refers to the phenomenon where the characteristics of the research subject may show different results when observed or analyzed at different scales. The environmental factors selected in this study may have a high degree of explanation for land use distribution at one spatial scale but not at another. This study selected four different spatial scales as alternative research scales, respectively calculating the average values of the environmental factors and the area proportion of land use types at each scale.

Due to the large number of factor types, principal component regression analysis was chosen as the evaluation method. Principal component regression analysis is a method that combines principal component analysis (PCA) and linear regression. It involves dimensionality reduction of the predictor variables through PCA and then using them as independent variables in regression analysis [34,35]. The principal component analysis formula is as follows:

$$X_{std} = Standardize(X) \quad (4)$$

$$C = Covariance(X_{std}) \quad (5)$$

$$C = V\Lambda V^T \quad (6)$$

In the above formulas,  $X_{std}$  is the matrix of the standardized predictor variables,  $C$  is the covariance matrix,  $V$  is the matrix of eigenvectors, and  $\Lambda$  is the diagonal matrix of eigenvalues.

The regression analysis formula is as follows:

$$Y = \beta_0 + B^T PC + \varepsilon \quad (7)$$

In the above formula,  $Y$  is the response variable,  $\beta_0$  is the intercept,  $B$  is the coefficient of the principal components,  $PC$  is the principal component score, and  $\varepsilon$  is the error term.

Based on the regression formulas for each land use type, the distribution of each land use type within the study area is calculated using the Spatial Analyst tool in ArcGIS software, combined with the  $R$  values obtained from the principal component analysis to select the most appropriate research scale.

After determining the research scale, the correlation between the two sets of data is calculated through correlation analysis. Correlation analysis is the main statistical method we used to explore the relationships between research variables. By calculating the Pearson correlation coefficient, we can quantify the strength and direction of the linear relationship between variables. The value of the Pearson correlation coefficient ranges from  $-1$  to  $1$ , where  $-1$  indicates a perfect negative correlation,  $1$  indicates a perfect positive correlation, and  $0$  indicates no linear relationship [36,37]. The correlation analysis in this study is implemented using the ggplot2 package in the R language.

The specific calculation formula is:

$$r = \frac{n(\sum xy) - (\sum x)(\sum y)}{\sqrt{(n\sum x^2 - (\sum x)^2)(n\sum y^2 - (\sum y)^2)}} \quad (8)$$

Here,  $x$  and  $y$  are the values of the two variables, and  $n$  is the number of observations.

### 2.6. Adaptive Atlas Based on Multi-Criteria Evaluation

Multi-Criteria Evaluation (MEC) is an evaluation method that integrates the impact of multiple factors. This study, through the correlation analysis of various land use types and natural environmental factors as well as the study of their interval distribution charac-

teristics, comprehensively analyzes the suitability of different factors for land use types, determines the fitting curves between them, and ultimately constructs data layers for the suitability of each land use type through overlay analysis [38–40]. This step is carried out using IDRISI software. Taking cultivated land as an example, a predictive probability map for cultivated land is created under the decision wizard tool. Water bodies are input as restrictive factors for the prediction, while elements such as elevation and slope are input as influencing factors. The function curves and weights for each influencing factor are set to generate a predictive layer for cultivated land. Finally, all predictive layers are merged using the Collection Editor tool to create the MEC atlas.

### 2.7. Cellular Automata Model

Cellular Automata (CA) is a complex dynamical model with discrete time, space, and state. Cells represent individual units within the whole, where the state of a cell at time  $t$  determines its state at time  $t + 1$ . By establishing rules for cell state transformation and defining the cellular neighborhood, the evolution of land use types can be dynamically simulated [23].

$$S_{t+1} = f(S_t, N) \quad (9)$$

In the above formula,  $S_t$  and  $S_{t+1}$  represent the states of the cell at different times;  $f$  is the rule for cell state transformation;  $N$  is the cellular neighborhood.

### 2.8. CA-Markov Model Computation

In this study, the computation of the CA-Markov model is conducted on the IDRISI platform to predict future land use patterns in the study area [41]. We selected land use data from 2015 and 2020 as the bases for our study. The time interval was set to 5 years, and the error rate was fixed at 0.15. This approach enabled us to obtain data on land use area transitions and transition probabilities between different land use types in the Ganjiang River basin from 2015 to 2020 [42]. Taking into account various natural and social factors of the study area, we constructed an MCE atlas based on different types of land use, which served as the operational rules for the cellular automaton. As the target forecast year for this study is 2040, we used land use data from 2020 as the base year. We then inputted the Markov computation results and the MCE atlas into the CA-Markov model, setting the cycle period to 10 years. This process ultimately allowed us to obtain the spatial pattern of land use in the Ganjiang River basin for the year 2040.

### 2.9. Kappa Coefficient for Model Validation

To ensure the accuracy of the predicted land use types in the Ganjiang River basin, this study employs Kappa validation to verify the model. Kappa validation is a commonly used statistical method in land classification accuracy assessment, primarily used to compare land use classification maps at different time points, thereby evaluating the accuracy of land use change models [13,43]. The formula for calculating the Kappa coefficient is:

$$K = \frac{P_o - P_e}{1 - P_e} \quad (10)$$

In the formula,  $K$  is the Kappa coefficient,  $P_o$  is the observed accuracy rate, i.e., the proportion of correctly classified instances, and  $P_e$  is the random accuracy rate, used to assess the probability of correct classification by chance.

This study first uses land use data from 2010 and 2015 as modeling objects. Through the aforementioned CA-Markov modeling process, a land use prediction model for 2010–2015 is constructed. Based on this model, the 2015 land use data is used as the prediction benchmark year to forecast the land use pattern for 2020. Finally, the results obtained from the model's prediction are validated against the actual land use data of 2020 using Kappa validation. This step is executed using the CROSSTAB tool in IDRISI software, where the predicted data and actual data are input to calculate the Kappa coefficient. In

previous studies, we considered a Kappa coefficient of 0.6 or above as indicative of good simulation results.

#### *2.10. Extraction of Key Areas in Land Use Evolution*

This study used the Identity tool in ArcGIS software to identify land use data from 2020 and 2000, calculating the areas where each land use type changed over 20 years. Observation of these results revealed that over 99% of the transferred plots are slender and small in area, mainly occurring at the edges of larger land plots. We believe that this phenomenon is due to reasonable errors generated during the identification process of land use data, and the impact of these plots should be ignored when counting key areas of land use evolution. Taking forest land a as an example, the number of plots transferred from forest land a to other land use types reached 903,449. By observing the morphology of the plots and their relationship with surrounding larger plots, we selected 1443 plots larger than 0.015 km<sup>2</sup> as the objects for extracting key areas of land evolution. After extracting valid plots, surface features were extracted based on different types of changes, converted into point features using the Feature To Point tool, and kernel density analysis was conducted using plot area as the population field, ultimately obtaining spatial distribution maps of different transfer phenomena.

### **3. Results**

#### *3.1. Environmental Factor Characteristics*

Analyzing the distribution characteristics of various factors in the study area and their impact on land use types is a crucial step in creating Multi-Criteria Evaluation (MCE) atlases. In this paper, Euclidean distances were calculated through buffer analysis on the ArcGIS platform, serving as key evaluation factors for the MCE atlas. The Ganjiang River basin's overall topographical features display a distinct pattern: low and flat in the north and high and steep in the south, indicating a high degree of spatial heterogeneity. Meteorological data for the basin were sourced from meteorological stations within and surrounding the study area. The spatial characteristics of various meteorological parameters within the basin were calculated using the ordinary Kriging interpolation method. The results reveal that temperatures in the southern part of the basin are generally higher, while the northern and western parts experience relatively lower temperatures. The annual average rainfall is higher in the west, north, and east, but lower in the south and central areas. The annual average total radiation exhibits a pattern of being higher in the south and lower in the north, with a relatively balanced distribution across the basin. Road factors were evaluated based on road buffer zones. Roads, railways, expressways, national highways, provincial roads, municipal roads, county roads, town roads, township roads, and village roads were categorized into three groups based on their characteristics and attributes. Railways and expressways were grouped together as one type; national highways, provincial roads, and municipal roads as another; and town roads, township roads, and village roads as the third category. The distribution characteristics of each evaluation factor in the Ganjiang River basin are illustrated in Figure 2. This comprehensive analysis provides a foundational understanding of the various factors influencing land use distribution, which is essential for the accurate creation of MCE atlases and subsequent land use planning and management.

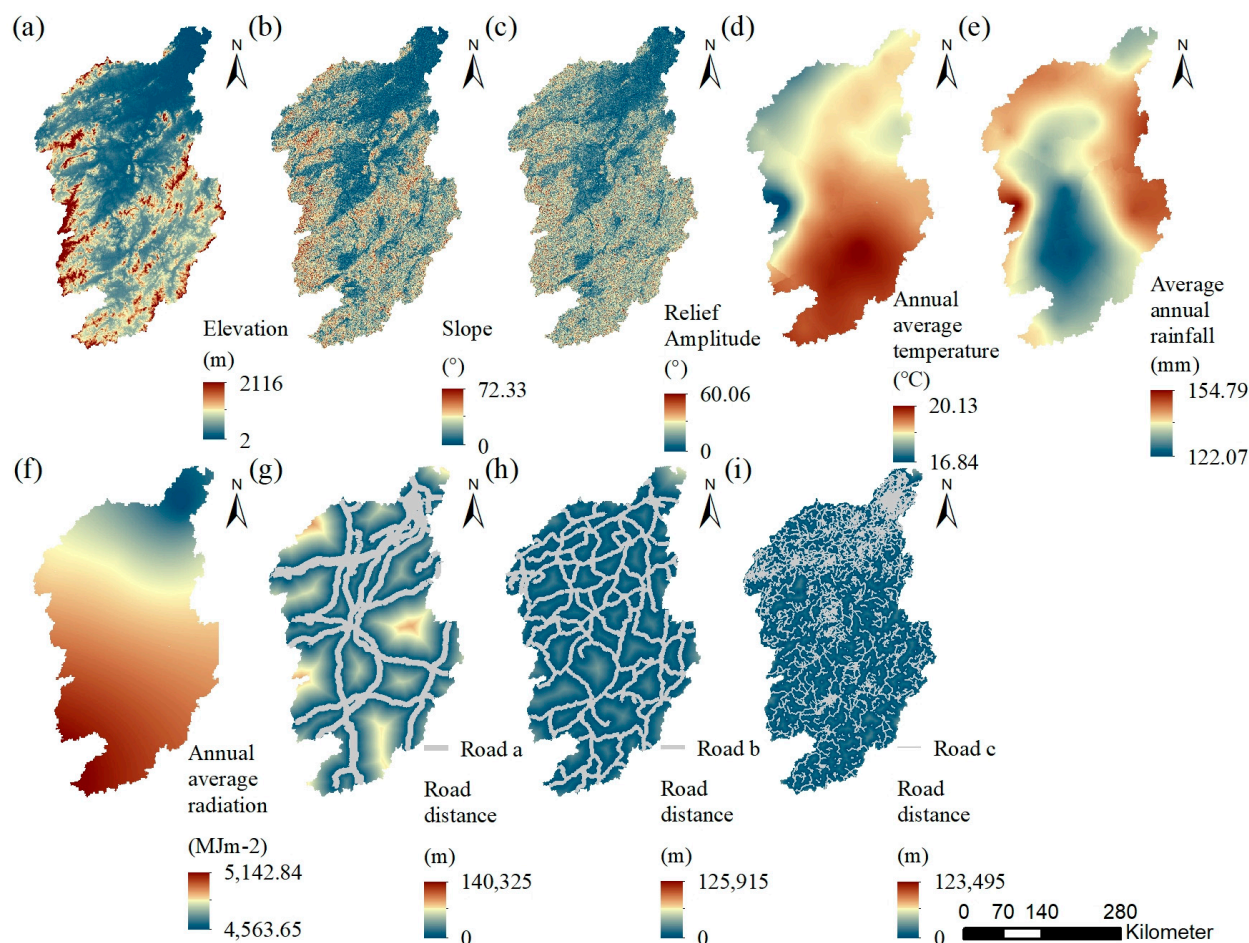


**Figure 2.** Distribution characteristics of various evaluation factors in the Ganjiang River.

### 3.2. Distribution and Change Characteristics of Subcategories of Forest Land

#### Divergence and Factor Detection

Figure 3 illustrates the distribution of land use types in the Ganjiang River basin from 2000 to 2020, highlighting a pattern where forest land is more abundant in the south and less so in the north. Among the forest land categories, type a has the most extensive distribution, predominantly found in high-altitude mountainous areas. Forest land type b is more concentrated around urban areas, especially in the southern Ganzhou region of the basin. In contrast, forest land type c, which covers a smaller area, is commonly found in the peripheral regions of construction land. Cultivated land is primarily located in the central and northern parts of the basin. In terms of water bodies and non-vegetated land use types, the Poyang Lake and various tributaries of the Ganjiang River are significant aquatic features of the study area. Construction land is mainly concentrated around urban centers.

Forest land is the dominant land use type in the Ganjiang River basin, accounting for 67.31% of the area in 2000, which then decreased slightly to 66.43% by 2020. Within the forest land categories, type a is the largest subcategory, with its area proportion fluctuating around  $49\% \pm 1\%$  over the past two decades. The area proportion of forest land type b has varied within  $13\% \pm 1\%$  during this period, while type c, the smallest subcategory, has remained around 5.5%, indicating overall low variation in area for all three subcategories. Cultivated land, the second largest land use type after forest land, has shown a declining trend in area over the 20-year period. Among non-vegetated land use types, water bodies and unused land have shown some fluctuation in proportion, but the overall magnitude is small and remains stable. However, there is a clear upward trend in the proportion of construction land, as detailed in Table 2.

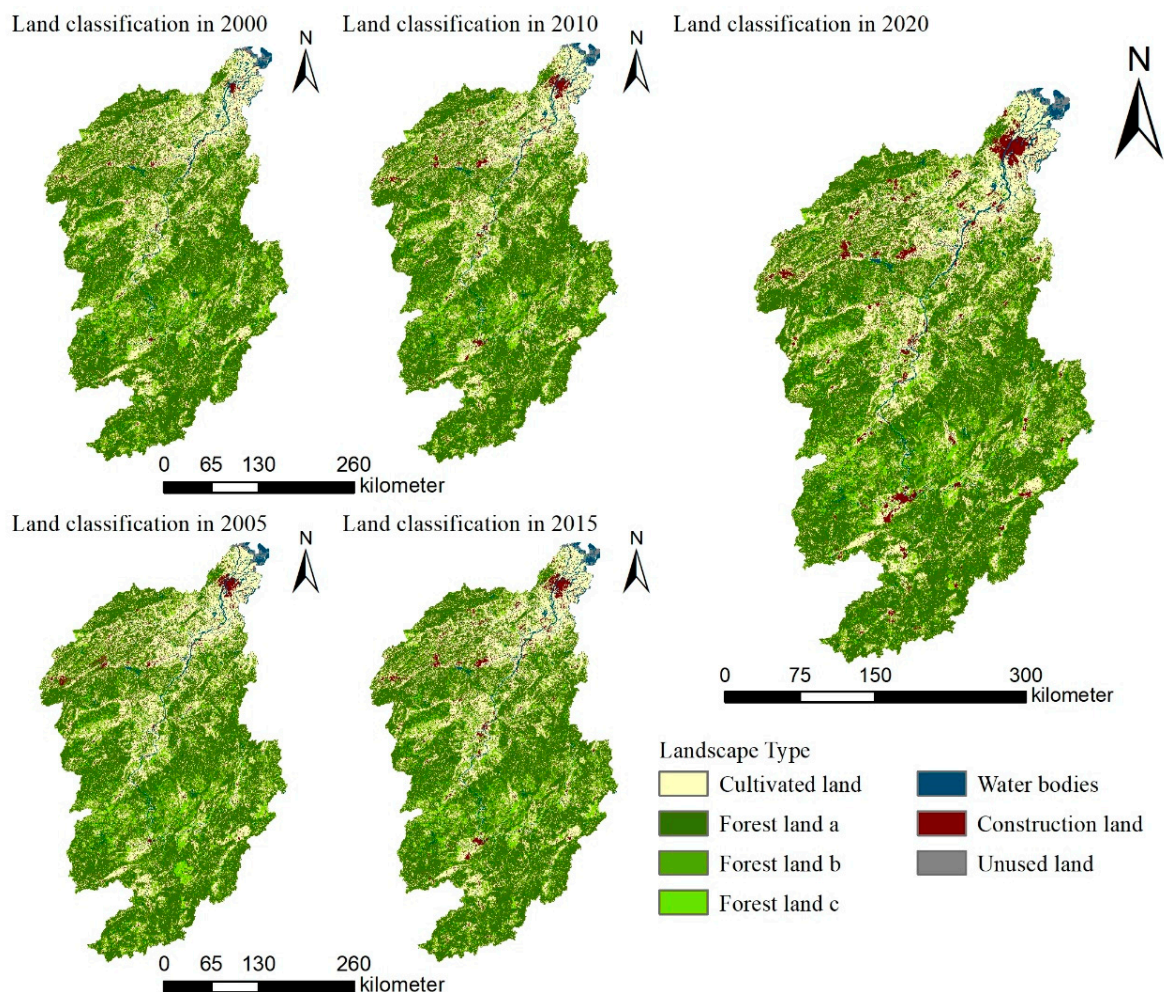


**Figure 3.** Distribution map of land use types in the Ganjiang River basin from 2000 to 2020.

**Table 2.** Proportion of land use types in the Ganjiang River basin from 2000 to 2020.

Years	Cultivated Land	All Types of Forest Land	Forest Land a	Forest Land b	Forest Land c	Water Bodies	Constructed Land	Unused Land
2000	26.44%	67.31%	48.25%	13.68%	5.38%	2.45%	1.81%	0.31%
2005	26.29%	67.10%	47.73%	13.69%	5.68%	2.41%	2.20%	0.31%
2010	26.27%	66.83%	48.49%	13.00%	5.34%	2.40%	2.49%	0.33%
2015	26.09%	66.68%	48.42%	12.94%	5.32%	2.40%	2.83%	0.32%
2020	25.72%	66.43%	47.93%	12.81%	5.68%	2.41%	3.43%	0.31%

### 3.3. Establishing the Research Scale for Correlation Analysis

This study employed four different research scales for analysis. Data sampling was conducted at these varying scales, focusing on patches where the average values of environmental factors within each patch and the area proportion of each land use type were calculated. These environmental factors served as the original variables for principal component analysis, resulting in four sets of principal component results (Tables 3 and 4).

From these, the first and second rotated components were chosen as the principal component regression factors. Among the four research scales, the county administrative division scale demonstrated the highest explanatory degree for land use types, with a cumulative value reaching 0.901. The small watershed scale followed with a cumulative value of 0.859, the 10 km grid scale had a value of 0.871, and the 1 km grid scale had the lowest value at 0.787. To further assess the explanatory degree of environmental factors on

the distribution of each land use type at different scales, principal component restoration was performed on the data from all four scales, yielding six regression formulas for each. Utilizing the Spatial Analyst tool in ArcGIS software, the distribution probability of each land use type on grid cells was calculated (Figure 4). The results indicated that at the 1 km grid scale, the restoration degree of land use type distribution was extremely poor, showing significant inconsistency with the actual distribution. Both the 10 km grid scale and the small watershed scale performed well in restoring the distribution of cultivated land, forest land type a, and construction land. However, these scales were less effective in accurately restoring forest land types b and c. The restoration degree at the administrative division scale was overall good and aligned with the expectations of this study.

**Table 3.** Results of principal component analysis at various research scales a.

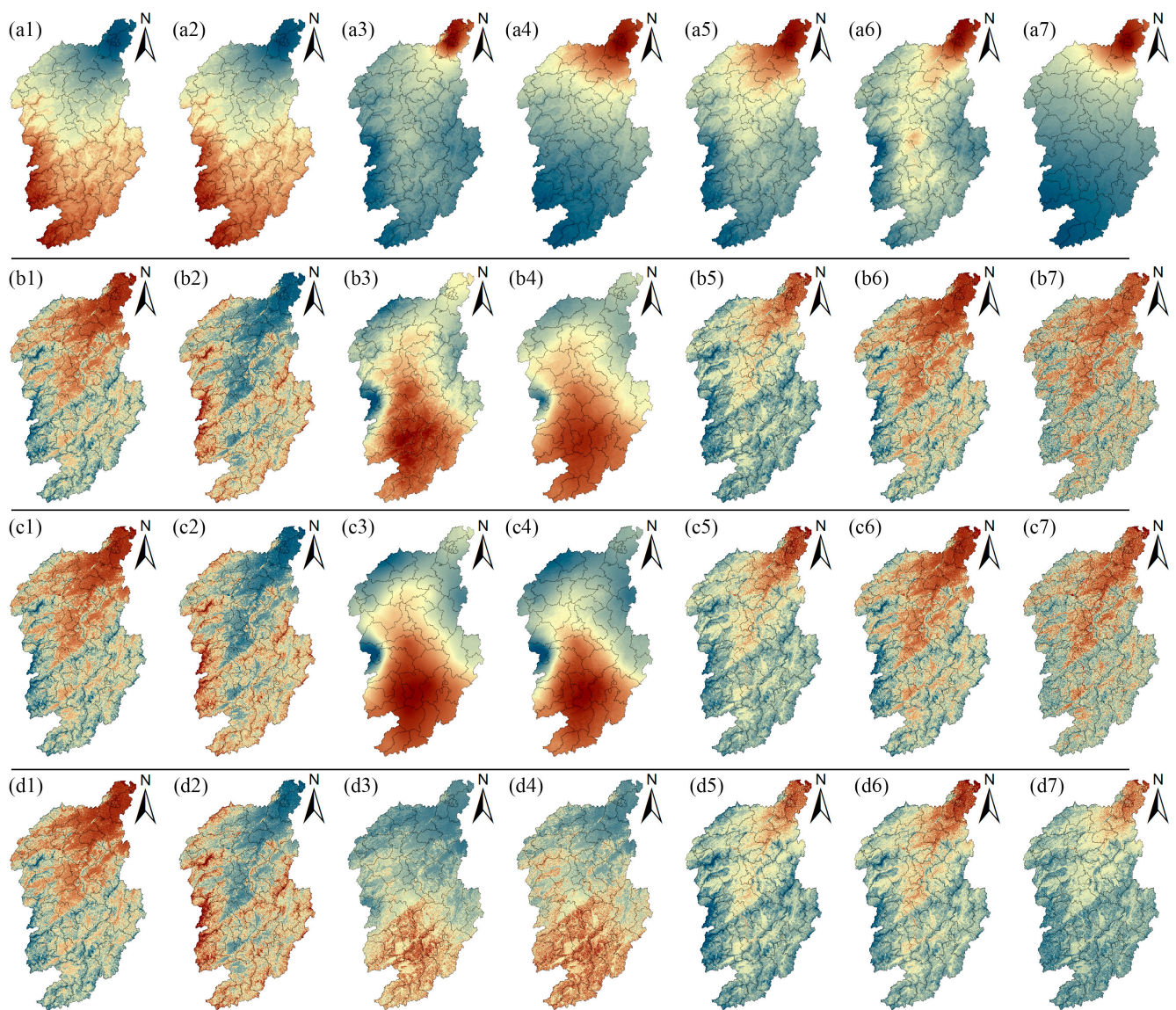
Environmental Factors	1 km Grid Scale						10 km Grid Scale					
	RC1	RC2	RC3	RC4	RC5	RC6	RC1	RC2	RC3	RC4	RC5	RC6
Annual average temperature	-0.239	0.528	-0.464	0.664	0.09	0.004	0.178	-0.613	0.477	0.594	0.109	0.004
Average annual rainfall	0.069	0.588	0.753	0.046	0.284	0	0.422	-0.32	0.348	-0.762	0.137	0.002
Annual average radiation	0.252	-0.56	0.218	0.632	0.419	0.002	-0.13	0.621	0.746	0.044	0.198	0.004
Elevation	0.521	0.089	0.153	0.327	-0.768	0	0.501	0.203	0.132	0.105	-0.824	-0.013
Slope	0.549	0.165	-0.272	-0.156	0.271	-0.707	0.511	0.218	-0.195	0.166	0.365	-0.702
Relief amplitude	0.549	0.164	-0.269	-0.162	0.269	0.707	0.511	0.219	-0.198	0.164	0.343	0.712

**Table 4.** Results of principal component analysis at various research scales b.

Environmental Factors	Small Watershed Scale						District and County Administrative Division Scale					
	RC1	RC2	RC3	RC4	RC5	RC6	RC1	RC2	RC3	RC4	RC5	RC6
Annual average temperature	0.21	-0.603	0.534	0.542	0.114	0.002	0.15	-0.66	0.569	0.44	0.157	0.006
Average annual rainfall	0.439	-0.296	0.266	-0.792	0.146	-0.003	0.463	-0.199	0.282	-0.816	-0.015	0
Annual average radiation	-0.125	0.631	0.729	-0.017	0.235	0.002	-0.062	0.673	0.724	0.048	0.128	0.004
Elevation	0.484	0.225	0.156	0.084	-0.827	0.01	0.501	0.14	0.037	0.279	-0.807	-0.013
Slope	0.507	0.224	-0.207	0.191	0.329	-0.711	0.504	0.162	-0.186	0.175	0.404	-0.701
Relief amplitude	0.507	0.222	-0.214	0.187	0.344	0.704	0.504	0.163	-0.191	0.173	0.38	0.713

### 3.4. Analysis of Environmental Factor Correlations and MCN Atlas Production

Correlation analysis was conducted to assess the relationship between six natural factors and seven types of land use. The analysis revealed that cultivated land and forest land type a have strong correlations with environmental factors. Water bodies and construction land also exhibit notable correlations, albeit to a lesser extent. In contrast, forest land types b and c as well as unused land demonstrate weaker correlations with these natural factors. Specifically, the correlation between cultivated land, forest land type a, and three groups of topographic factors (elevation, slope, and relief amplitude) is above 0.5. However, their correlation with rainfall factors is around 0.3. Temperature and radiation factors have a lower impact on these land use types. Water bodies and construction land show a correlation of above 0.2 with topographic factors and about 0.2 with rainfall factors (Figure 5). These findings indicate that topographic elevation, slope, undulation, and rainfall have significant impacts on cultivated land, forest land type a, water bodies, and construction land. Conversely, forest land types b and c and unused land are less influenced by these natural factors.



**Comparison of Principal Component Regression Results of Environmental Factors on Seven Types of Land Use at Different Research Scales**



**Figure 4.** Comparison of principal component regression results of environmental factors for seven types of land use at different research scales: the figure is horizontally divided into four rows, (a–d), representing different data extraction scales. (a) represents a 1 km grid as the research scale, (b) represents a 10 km grid as the research scale, (c) represents the small watershed research scale, and (d) represents the county administrative division research scale. Vertically, the figure is divided into columns (1–7), representing different types of land use. (1) represents cultivated land, (2) represents forest land a, (3) represents forest land b, (4) represents forest land c, (5) represents construction land, (6) represents water bodies, and (7) represents unused land. For example, (d1) illustrates the prediction of the distribution of cultivated land using the principal component regression formula at the county administrative division research scale [32,33,44].

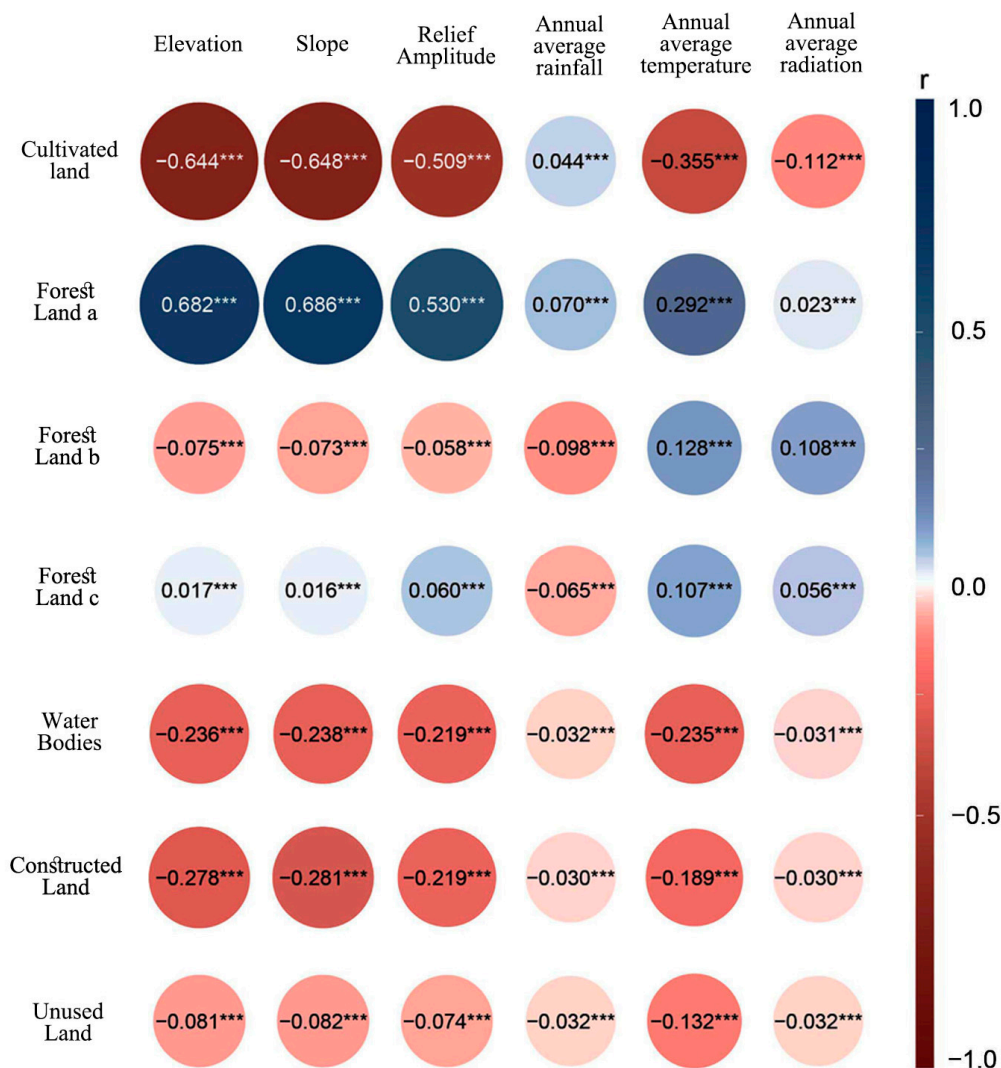


**Figure 5.** Correlation analysis between natural environmental factors and land use types: the indices inside the circles in the figure represent the Pearson correlation coefficients between the two factors on the x-axis and y-axis. The ‘+’ before the number indicates a positive correlation, while the ‘-’ indicates a negative correlation. The ‘\*’ following the number denotes the level of statistical significance, with ‘\*\*\*’ indicating  $p < 0.001$ , signifying a high level of significance.

In constructing the MCN atlas, this study ultimately selected factors such as elevation, slope, topographic relief, annual average temperature, and roads. Initially, restrictive factors were identified for each of the seven land use types. Based on the results of the correlation analysis, function curves were constructed for the target land types using various environmental factors. These curves were designed to simulate the potential suitability of land types within different value ranges of these environmental factors. Finally, the Analytic Hierarchy Process (AHP) method was employed to assign weights to different evaluation factors. In combination with the restrictive factors of land types, a land suitability layer was constructed (Figure 6).

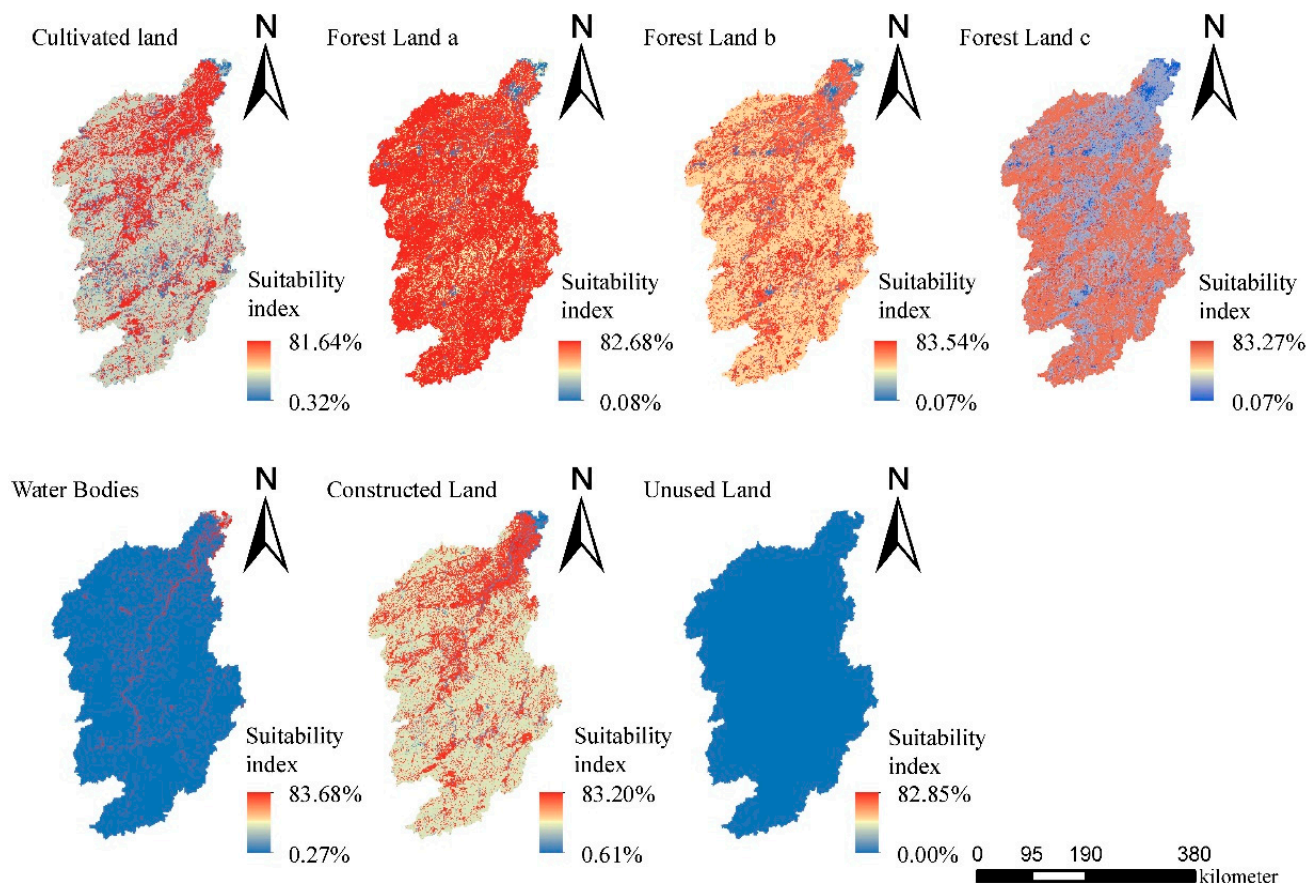


Figure 6. MCE adaptive atlas.

### 3.5. Prediction of Land Use Patterns in the Ganjiang River Basin

Using the CA-Markov model, the 2015 land use data were used as the baseline to predict the 2020 land use data. The results, verified by the kappa test, achieved an accuracy of 0.92, indicating a high level of model reliability [45,46]. The calculated land use data for 2040 in the Ganjiang River basin (Figure 7) show, compared to 2020, an increase in construction land area by 2188.8190 km<sup>2</sup>, a decrease in cultivated land area by 602.8985 km<sup>2</sup>, a decrease in forest land type a area by 1421.8400 km<sup>2</sup>, a decrease in forest land area by 1219.4700 km<sup>2</sup>, an increase in forest land type c area by 1060.5940 km<sup>2</sup>, an increase in water area by 39.5166 km<sup>2</sup>, and a decrease in unused land area by 45.1178 km<sup>2</sup> (Table 5).

Table 5. Characteristics of land use changes in the Ganjiang River basin from 2020 to 2040.

Data Name	Cultivated Land/km <sup>2</sup>	Forest Land a/km <sup>2</sup>	Forest Land b/km <sup>2</sup>	Forest Land c /km <sup>2</sup>	Water Bodies/km <sup>2</sup>	Constructed Land/km <sup>2</sup>	Unused Land/km <sup>2</sup>
Area in 2040	23,675.9369	44,306.1900	10,997.3300	6485.5560	2294.9690	5419.8550	242.6102
Change in area compared to 2020	−602.8985	−1421.8400	−1219.4700	1060.5940	39.5166	2188.8190	−45.1178

### 3.6. Analysis of Forest Land Transition Characteristics

Between 2000 and 2020, forest land type a was the most stable land use type, with the main transitions occurring between forest land types b and c. Forest land types b and c were the two most unstable land use types. Between 2005 and 2010, these two types transferred 6.73% and 7.91% of their area to forest land type a, respectively. In other periods, the holdings of forest land types b and c were also significantly lower than those of forest land type a (Figure 8).

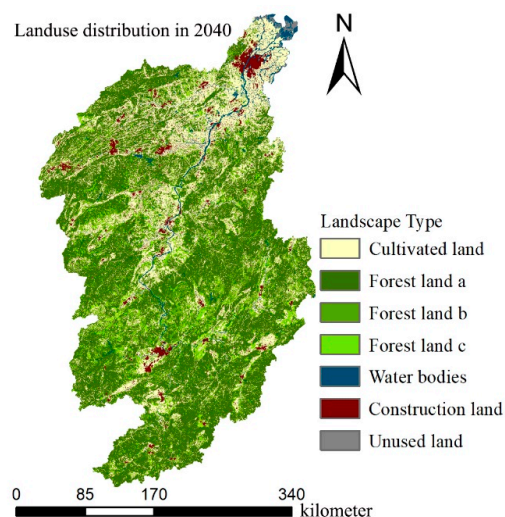


Figure 7. Prediction of land use distribution in the Ganjiang River basin in 2040.

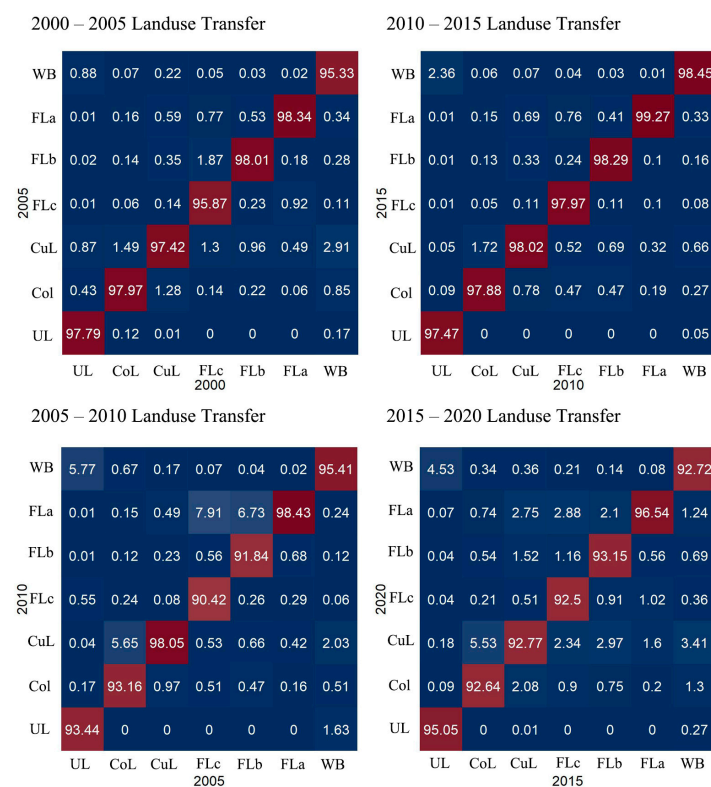
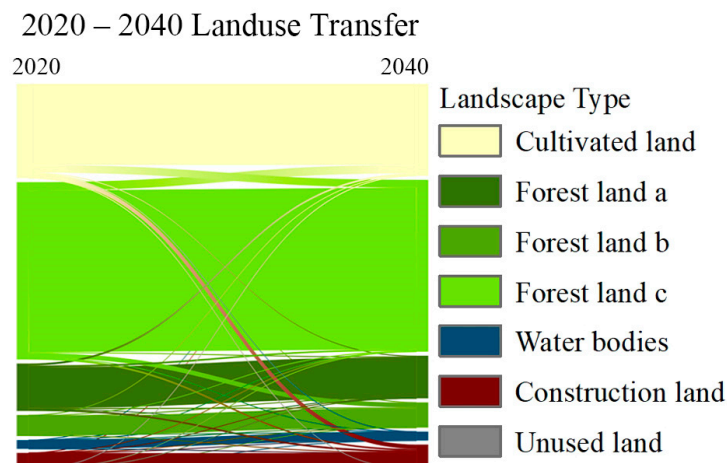


Figure 8. Land use type transition matrix in the Ganjiang River basin from 2000 to 2020: The numbers in the graph represent the conversion probability from the horizontal axis element to the vertical axis element, with the unit being percentage. The color of the number’s background indicates the value level, with red representing high and blue representing low.

Between 2020 and 2040, changes in land types were mainly concentrated around rivers and major cities. In plain areas, the increase in construction land area and the decrease in agricultural land area were quite evident, while changes in hilly and mountainous areas were relatively stable; the area of forest land type a showed an increasing trend in high-altitude, steep-slope terrains, with a significant amount of area being transferred to forest land type c in low-altitude areas; forest land type b exhibited a decreasing trend in all areas, with the main direction of transition being towards construction land; the area of forest land type c increased in hilly and mountainous regions (Figure 9).



**Figure 9.** Land transition directions in the Ganjiang River basin from 2020 to 2040.

#### 4. Discussion

##### 4.1. Analysis of Land Use Change Characteristics from 2000 to 2020

Over the past two decades, the Ganjiang River basin has experienced significant changes in land use. From 2000 to 2020, the total forest land area in the basin decreased by 0.88%. Among the forest land subcategories, forest land type a decreased by 0.32%, type b by 0.87%, while type c increased by 0.30%. This indicates that types b and a are primarily responsible for the overall decrease in forest land area. The land use area transition matrix reveals that 8.16% of forest land type b converted to type a over this period. Additionally, 2.96% of type b transitioned to cultivated land, while construction land and forest land type c accounted for 1.73% and 1.14% of the total area of type b, respectively. Over the same period, the main transfers from forest land type a included cultivated land (1.65%), forest land type c (1.4%), type b (1.13%), and construction land (0.59%). In terms of area transfer, over 20 years, the land types most frequently converting into forest land type c were primarily types a and b, with other land types contributing less than 0.5%. The interval from 2005 to 2010 witnessed the most dramatic changes in the area of various forest land subcategories. During this period, the vast majority of forest land types c and b remained stable, with their area proportions being 90.42% and 91.84%, respectively.

To further analyze the transfer characteristics of forest land subcategories in the Ganjiang River basin over 20 years, we overlaid the 2000 land use data with that of 2020, identifying key areas of transfer for the three forest land types (Figure 10). The results show that transfers from forest land a to cultivated land were infrequent. Transfers from forest land a to type b were mainly concentrated in the southern part of Ganzhou City, especially in Longnan County, where over 170 km<sup>2</sup> of land transferred in 20 years. Significant transfers to type b also occurred in the southern basin areas of Yudu County, Xingguo County, and Ningdu County, predominantly in areas with altitudes of 300–400 m. These transfers were characterized by large and concentrated plots, distributed along areas with high topographic relief. In the southern parts of Nankang District and Zhanggong District, where urbanization levels are higher, many transfers occurred around 200 m altitude, with relatively smaller and more scattered plots. Transfers from forest land a to type c were mainly concentrated in the northwestern basin areas of Lianhua County and Yongxin County and in the southern areas of Yudu County and Shicheng County, occurring at altitudes of around 400 m. Transfers from forest land a to construction land did not exhibit distinct characteristics, with this study recording only seven valid transfer plots, each less than 0.05 km<sup>2</sup> in area.

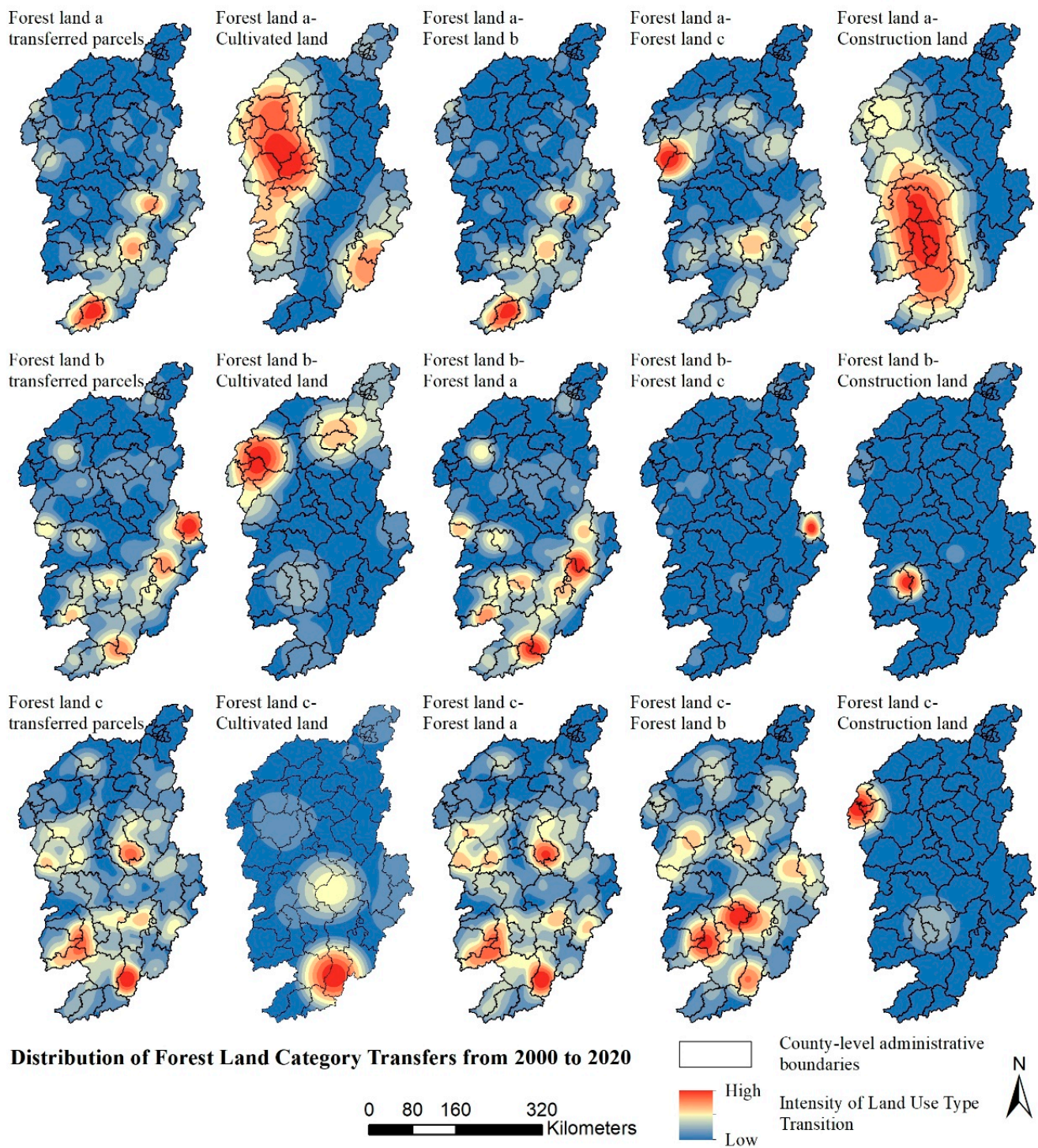


**Figure 10.** Distribution of forest land category transfers from 2000 to 2020.

Transfers from forest land type b to cultivated land were relatively infrequent, primarily occurring in Luxi County, located in the northwestern part of the basin. The transitions from forest land type b to type a were notably concentrated in Ningdu County, Anyuan County, and Dingnan County in the southern part of the basin, characterized by overall large plot sizes. Notably, eight transfer plots exceeded 5 km<sup>2</sup> in area and were geographically concentrated. Several significant transfer plots appeared around major urban areas, including Xinjian District in Nanchang City, Yuanzhou District in Pingxiang City, and Ganzhou District, Zhanggong District, and Nankang District in Ganzhou City. Over 60%

of the transfers from forest land type b to type c were focused in Guangchang County in the eastern part of the basin. Transfers from forest land type b to construction land were relatively rare, mainly occurring in Shangyou County in the southern part.

The transfer of forest land type c to arable land is concentrated in Dingyuan County in the southern part and Xingguo County in the central part, predominantly occurring in valley and basin areas. The transition of forest land type c to forest land type a is widespread. This transition occurs in all areas except for the northern plains of the basin and is concentrated in the central and southern regions, with the transfer patches often located in areas of relatively higher elevation. The transition from forest land type c to forest land type b is focused in Ganzhou District and Nankang District in the southern part of the basin. The transition of forest land type c to construction land occurs in the Xiangdong District area in the northwest.

From 2000 to 2020, the most significant phenomenon in the Ganjiang River basin was the transfer of land between various subcategories of forest land, with the main phase of these transfers occurring between 2005 and 2010. During this period, significant land activities were observed in the southern part of the basin, particularly in Yudu, Longnan, and Dingnan counties. In addition to forest land, construction land and arable land are notable for their significant changes. Over these 20 years, the proportion of construction land in the basin increased from 1.81% to 3.43%, while arable land decreased from 26.44% to 25.72%, with arable land primarily being converted into construction land.

The Ganjiang River basin is characterized by spatial heterogeneity in its terrain, featuring plains in the central and northern areas and hills and mountains in the southwest. Among the three subcategories of forest land focused on in this study, the spatial distribution of forest land type a is closely related to the terrain. Although forest land types b and c exhibit a weaker correlation with terrain, the changes in their area proportions across different elevational zones are significant. The mutual conversion between different forest land subcategories is more frequent in areas with high terrain undulation, particularly in the southern part of the basin where transfer patches are larger and more intact. In contrast, the central area features more fragmented transfer patches, and transfers are less frequent in the northern plains.

#### *4.2. Land Use Transition Characteristics and Key Areas of Forest Land Subcategory Transitions in 2040*

Based on the 2040 land use pattern prediction results, it was found that the growth of construction land is the main cause of land use changes. From 2000 to 2040, the area of construction land increased by 2188.8190 km<sup>2</sup>, the largest change among the seven land use types, while the largest decreases in area were in forest land a, forest land b, and cultivated land, in that order. Among the land use types converted to construction land, cultivated land had the largest area, reaching 2021.9622 km<sup>2</sup>. The area of converted forest land a was 691.6243 km<sup>2</sup>, forest land b was 673.7042 km<sup>2</sup>, and forest land c was 276.5588 km<sup>2</sup>. Overall, from 2020 to 2040, the land type changes showed a transfer pattern from forest land to cultivated land to construction land. Cultivated land around major urban areas was converted to construction land due to urban expansion, while nearby forest land further transformed into cultivated land to supplement the agricultural resources of the regions. This phenomenon aligns with the objective needs of urban expansion in the Ganjiang River basin and China's strict policies on cultivated land protection, conforming to the objective laws of social development.

Overlaying the predicted 2040 land use data with the actual data from 2020, we analyzed the transfer distribution of different subcategories of forest land over 20 years (Figure 11). The largest transfer area from forest land a to cultivated land was mainly concentrated in the northern part of the basin and Zhanggong District in the south, all at the edges of urban areas. The transfer from forest land a to cultivated land was primarily distributed in the central and northern parts of the basin; the transfer to forest land b was in the southern part of the basin; the transfer to forest land c was more evenly distributed

but mainly in plains or basin areas; the transfer to construction land was more concentrated in the urban areas of Nanchang, Yichun, and Ganzhou. The transfers from forest land b were more concentrated in the southern part of the basin, with the largest transfer area from forest land b to forest land a, mainly occurring in the south. Transfers from forest land b to cultivated land were distributed in the central and northern plains and the basin area of Longnan County in the south; transfers to forest land a were concentrated in Longnan County, Yudu County, Ningdu County, etc.; transfers to forest land c were more concentrated in the central area of Ji'an City and Yudu County; transfers to construction land were distributed around several major cities. The transfer phenomenon of forest land c, besides being concentrated around major urban areas, also had significant distribution in Guangchang County in the east and Lianhua County in the west. Transfers from forest land c to cultivated land were concentrated in the southern part of the basin; transfers to forest land a were concentrated in the high-altitude areas in the west; transfers to forest land b mainly occurred in Guangchang County in the west; transfers to construction land were more distributed around major cities.

Overall, transfers occur predominantly around major cities, with similar transfer characteristics between forest land a and forest land b. Transfers involving forest land c are relatively smaller in area and more scattered. Ji'an City, as the second largest city in the basin, experiences a much lower degree of land type changes around its urban area compared to Nanchang, Ganzhou, Yichun, and other places, which may be related to the flat terrain and relatively fewer transferable forest lands locally. The transfer of forest and cultivated lands to construction land is an inevitable phenomenon of social development, which may intensify in the next 20 years. This poses a severe challenge to the ecosystem. Strengthening the development from forest lands b and c to forest land a and scientifically enhancing the quality of existing forest lands might be an important approach to resolving land use conflicts [47].

#### 4.3. Ganjiang River Basin Forest Land Conservation Strategy

Our research highlights a concerning trend in the Ganjiang River basin of a continuous decline in forest land area over the past 20 years, with projections suggesting this decline may intensify by 2040. Moreover, studies have shown that the carbon storage in forest lands surrounding large cities in the northern part of the basin, such as Nanchang, will significantly decrease by 2040 [48]. This reduction in forest land not only poses a threat to biodiversity and ecosystem services [49,50], but also increases the risk of soil erosion. In China, stringent policies are in place to protect arable land [51]. Consequently, land that was reforested due to abandonment along with forest land in low mountain and gentle slope areas often revert to arable land following land consolidation. This process leads to a forest-to-cropland conversion. If the transition pattern of forest land-to-arable land-to-construction land becomes widespread, forest land indirectly contributes to the expansion of construction land. This trend complicates efforts to restore forest land area and poses a significant threat to the ecological security of the basin.

As of 2022, Jiangxi Province boasts a forest coverage rate of over 60%, demonstrating substantial potential for forest land conservation [52]. Ecological restoration projects [53] and policy management measures [54] have shown effectiveness in enhancing a region's ecological environment. In the Ganjiang River basin, a core area of Jiangxi Province, there is a critical need to implement relevant ecological projects and guide forest land restoration through policy interventions [55]. When the primary objective of forest land restoration is to bolster ecosystem services rather than economic gains, the focus should be on cultivating native species. This approach involves carefully selecting suitable sites and restoration measures based on scientific planning [56–58]. In scenarios where timber production or agroforestry economy is considered, it is vital to strike a balance between environmental and economic outcomes [59]. This balance necessitates tailored restoration strategies for different plots [60] and rational land planning to prevent the encroachment of production

of forest land on other forest areas [61]. Therefore, the initial focus of forest land restoration should be on determining the most appropriate locations for restoration efforts [62,63].

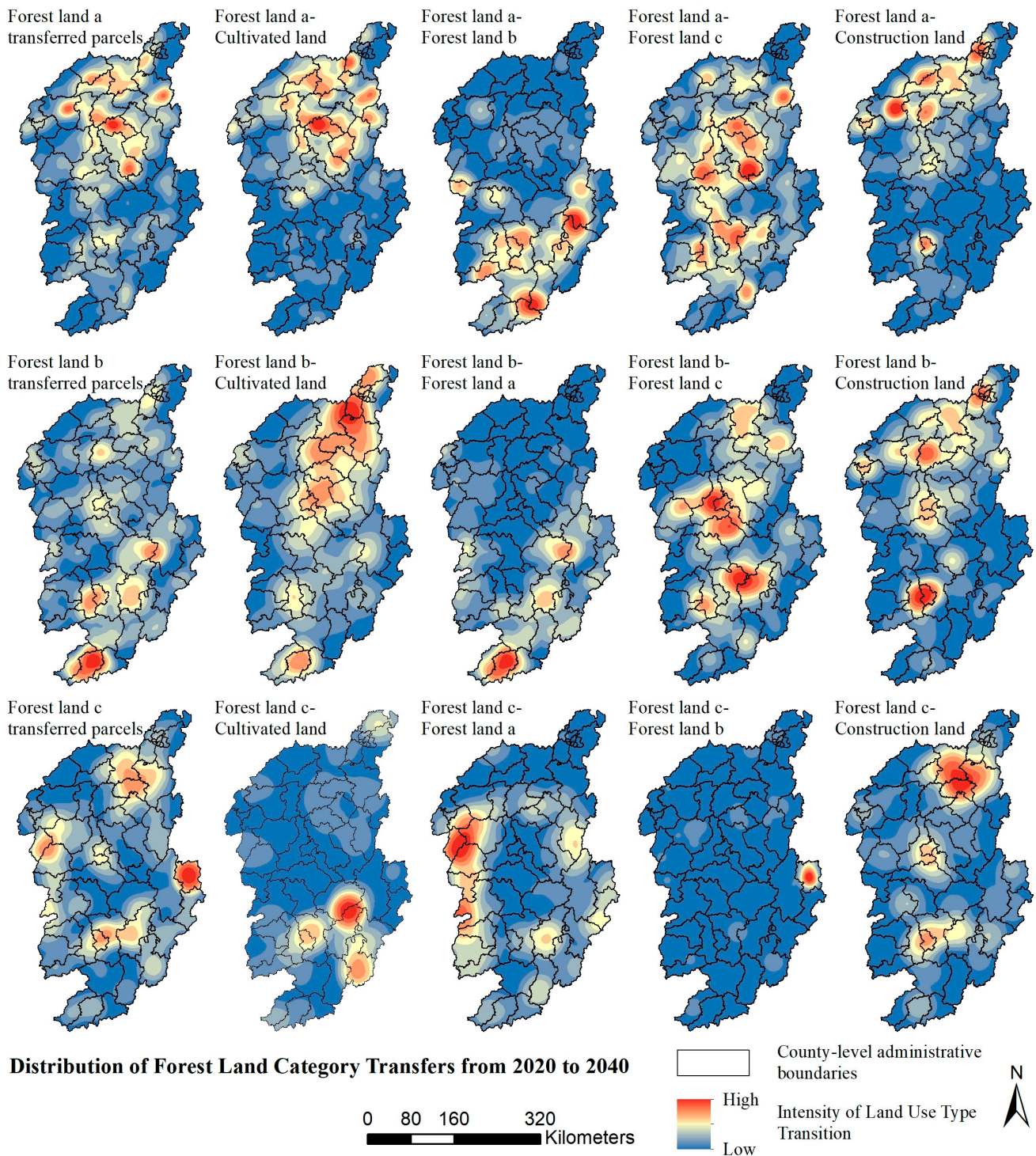


**Figure 11.** Distribution of forest land category transfers from 2020 to 2040.

Our study reveals that, over the past 20 years, the transition from forest land type a to types b and c has predominantly occurred in the southern and northwestern regions of the basin. Key areas of transition include Longnan, Yudu, Xingguo, Ningdu, Lianhua, and Yongxin counties. This shift from type a to types b and c is indicative of a decrease in forest canopy density. Moreover, certain transitions from type a to type c represent a shift in land

use from forest land to productive orchards. These areas, particularly those with significant land transitions in the past 20 years, have potential for forest land restoration and should be prioritized in restoration projects. In the next 20 years, the central part of the basin is also at risk of forest land type transitioning to other subcategories of forest land, and we need to prevent similar occurrences in this area through planning and policy measures. Furthermore, in recent years, Jiangxi Province has focused on developing local specialty economic forest products, leading to the transformation of some low-yield forest lands into economic forests. Agricultural products such as navel oranges, pomelos, and oil tea have become significant industries in the southern part of Ganzhou city in the basin. In the land planning of the Ganjiang River basin, we should consider the space for agricultural and forestry economic development, guiding the overall societal progress in a stable and positive direction.

#### 4.4. Uncertainty and Limitations

This paper provides an analysis of land use changes from 2000 to 2020 in the Ganjiang River basin and offers predictions for the distribution and changes of land use in 2040. It investigates the main reasons for the decrease in the area of various subcategories of forest land and proposes suggestions for the direction and methods of forest land restoration. However, there are still some uncertainties and limitations in this study that need to be addressed.

Firstly, the environmental elements used in predicting land use patterns in this paper encompass 10 items, primarily focusing on natural factors. The impact of related policies, however, has not been included in our study. This exclusion is due to the challenges in quantifying relevant policies for research purposes and the difficulties associated with collecting and filtering policy information. Secondly, the CA-Markov model, a method employed for predicting future scenarios, is based on the change characteristics observed between two time points. In our study, the data from 2015 to 2020 form the bases for predicting the 2040 land use pattern. However, this approach does not account for the impact of land use change characteristics in the study area from 2000 to 2015, and this omission could affect the comprehensiveness of our predictions. Finally, our prediction results suggest an increase in the area of construction land in the Ganjiang River basin, indicating further urban expansion. This projection is in contrast with the current trends in Chinese society, such as the slowdown in population growth [64] and the possibility of urban population shrinkage in the future [65]. Therefore, the validity of our prediction results in accurately reflecting future scenarios remains uncertain and warrants further investigation.

## 5. Conclusions

This paper analyzes the transfer characteristics of forest land and its subcategories in the Ganjiang River basin from 2000 to 2020. It finds that the mutual conversion between various subcategories of forest land is the most significant type of land use change. The southern part of the basin, predominantly mountainous and forested terrain, has experienced the greatest extent of land use changes over the past 20 years, primarily occurring in higher elevation areas. Among these, Yudu and Longnan counties have seen the most intense forest land transitions, with widespread decline in forest canopy density. In contrast, the northern part of the basin has not witnessed significant forest land transfers. Looking at the land use pattern predictions for 2040, from 2020 to 2040, the overall land use pattern of the basin will remain stable. Changes in land use are concentrated around large construction land patches. The land transfer phenomenon from forest land to arable land to construction land is particularly prominent. The expansion of construction land necessitates the transformation of nearby arable land patches, while forest land patches at the edges of arable land further convert to arable land. This phenomenon mainly occurs in the urban fringe areas of central cities such as Nanchang, Ganzhou, Yichun, and Ji'an. Compared to the land use changes between 2000 and 2020, the focus of land use evolution in the next 20 years may shift from the southern to the central and northern parts of the

basin, with urban expansion possibly becoming the main driving force of land use change during this period. Relative to strict controls on urban expansion, forest land restoration is a more effective method to compensate for the loss of forest land area. Key areas for forest land restoration work include Longnan, Yudu, Xingguo, Ningdu, Lianhua, and Yongxin counties in the southern and northwestern parts of the basin. Furthermore, terrain becomes the dominant natural factor influencing land use change and restricting urban expansion, highlighting the strong spatial heterogeneity of the terrain in the Ganjiang River basin. This also emphasizes the importance of adapting to local conditions in future regional planning.

**Author Contributions:** Conceptualization, Y.Z.; methodology, Y.Z.; software, Y.Z.; validation, Y.Z.; formal analysis, Y.Z.; investigation, Y.Z., G.X. and M.L.; resources, Y.Z. and M.L.; data curation, Y.Z. and J.H.; writing—original draft preparation, Y.Z. and J.H.; writing—review and editing, Y.Z. and J.H.; visualization, Y.Z.; supervision, Y.Z.; project administration, Y.Z. and M.L.; funding acquisition, M.L. All authors have read and agreed to the published version of the manuscript.

**Funding:** Jiangxi Province University Humanities and Social Sciences Research Project (JC22245).

**Data Availability Statement:** The data presented in this study are available on request from the corresponding authors.

**Conflicts of Interest:** The authors declare no conflicts of interest.

## References

- Subedi, P.; Subedi, K.; Thapa, B. Application of a Hybrid Cellular Automaton—Markov (CA-Markov) Model in Land-Use Change Prediction: A Case Study of Saddle Creek Drainage Basin, Florida. *Appl. Ecol. Environ. Sci.* **2013**, *1*, 126–132. [CrossRef]
- Ali, H. Land Use and Land Cover Change, Drivers and Its Impact: A Comparative Study from Kuhar Michael and Lenche Dima of Blue Nile and Awash Basins of Ethiopia. Doctoral Dissertation, Cornell University, Ithaca, NY, USA, 2009.
- Guo, J.; Yu, Z.; Ma, Z.; Xu, D.; Cao, S. What Factors Have Driven Urbanization in China? *Environ. Dev. Sustain.* **2022**, *24*, 6508–6526. [CrossRef]
- Singh, S.K.; Mustak, S.; Srivastava, P.K.; Szabó, S.; Islam, T. Predicting Spatial and Decadal LULC Changes Through Cellular Automata Markov Chain Models Using Earth Observation Datasets and Geo-Information. *Environ. Process.* **2015**, *2*, 61–78. [CrossRef]
- China | Population: Urbanization Rate | CEIC. Available online: <https://www.ceicdata.com/en/china/population-urbanization-rate> (accessed on 19 January 2024).
- Mokarram, M.; Pham, T.M. CA-Markov Model Application to Predict Crop Yield Using Remote Sensing Indices. *Ecol. Indic.* **2022**, *139*, 108952. [CrossRef]
- Zhao, M.; He, Z.; Du, J.; Chen, L.; Lin, P.; Fang, S. Assessing the Effects of Ecological Engineering on Carbon Storage by Linking the CA-Markov and InVEST Models. *Ecol. Indic.* **2019**, *98*, 29–38. [CrossRef]
- Yang, X.; Zheng, X.-Q.; Chen, R. A Land Use Change Model: Integrating Landscape Pattern Indexes and Markov-CA. *Ecol. Model.* **2014**, *283*, 1–7. [CrossRef]
- Dezhkam, S.; Jabbarian Amiri, B.; Darvishsefat, A.A.; Sakieh, Y. Performance Evaluation of Land Change Simulation Models Using Landscape Metrics. *Geocarto Int.* **2017**, *32*, 655–677. [CrossRef]
- Omar, N.Q.; Sanusi, S.A.M.; Hussin, W.M.W.; Samat, N.; Mohammed, K.S. Markov-CA Model Using Analytical Hierarchy Process and Multiregression Technique. *IOP Conf. Ser. Earth Environ. Sci.* **2014**, *20*, 012008. [CrossRef]
- Fu, F.; Deng, S.; Wu, D.; Liu, W.; Bai, Z. Research on the Spatiotemporal Evolution of Land Use Landscape Pattern in a County Area Based on CA-Markov Model. *Sustain. Cities Soc.* **2022**, *80*, 103760. [CrossRef]
- Zhou, L.; Dang, X.; Sun, Q.; Wang, S. Multi-Scenario Simulation of Urban Land Change in Shanghai by Random Forest and CA-Markov Model. *Sustain. Cities Soc.* **2020**, *55*, 102045. [CrossRef]
- Aburas, M.M.; Ho, Y.M.; Pradhan, B.; Salleh, A.H.; Alazaiza, M.Y.D. Spatio-Temporal Simulation of Future Urban Growth Trends Using an Integrated CA-Markov Model. *Arab. J. Geosci.* **2021**, *14*, 131. [CrossRef]
- Mansour, S.; Al-Belushi, M.; Al-Awadhi, T. Monitoring Land Use and Land Cover Changes in the Mountainous Cities of Oman Using GIS and CA-Markov Modelling Techniques. *Land Use Policy* **2020**, *91*, 104414. [CrossRef]
- Huang, Y.; Yang, B.; Wang, M.; Liu, B.; Yang, X. Analysis of the Future Land Cover Change in Beijing Using CA-Markov Chain Model. *Environ. Earth Sci.* **2020**, *79*, 60. [CrossRef]
- Hu, S.; Chen, L.; Li, L.; Zhang, T.; Yuan, L.; Cheng, L.; Wang, J.; Wen, M. Simulation of Land Use Change and Ecosystem Service Value Dynamics under Ecological Constraints in Anhui Province, China. *Int. J. Environ. Res. Public Health* **2020**, *17*, 4228. [CrossRef]
- Kiziridis, D.A.; Mastrogianni, A.; Pleniou, M.; Tsiftsis, S.; Xystrakis, F.; Tsiripidis, I. Improving the Predictive Performance of CLUE-S by Extending Demand to Land Transitions: The Trans-CLUE-S Model. *Ecol. Model.* **2023**, *478*, 110307. [CrossRef]

18. Wei, Z.; Liu, Y. Construction of Super-Resolution Model of Remote Sensing Image Based on Deep Convolutional Neural Network. *Comput. Commun.* **2021**, *178*, 191–200. [[CrossRef](#)]
19. Zeshan, M.T.; Mustafa, M.R.U.; Baig, M.F. Monitoring Land Use Changes and Their Future Prospects Using GIS and ANN-CA for Perak River Basin, Malaysia. *Water* **2021**, *13*, 2286. [[CrossRef](#)]
20. Legdou, A.; Amine, A.; Lahssini, S.; Chafik, H.; Berrada, M. Predicting Forest Cover Change in Middle Atlas Morocco: A Logistic-CA-Markov Approach. In *Proceedings of the Computer Vision and Robotics*; Bansal, J.C., Engelbrecht, A., Shukla, P.K., Eds.; Springer: Singapore, 2022; pp. 229–239.
21. Guan, D.; Zhao, Z.; Tan, J. Dynamic Simulation of Land Use Change Based on Logistic-CA-Markov and WLC-CA-Markov Models: A Case Study in Three Gorges Reservoir Area of Chongqing, China. *Environ. Sci. Pollut. Res.* **2019**, *26*, 20669–20688. [[CrossRef](#)]
22. Al-Hameedi, W.M.M.; Chen, J.; Faichia, C.; Nath, B.; Al-Shaibah, B.; Al-Aizari, A. Geospatial Analysis of Land Use/Cover Change and Land Surface Temperature for Landscape Risk Pattern Change Evaluation of Baghdad City, Iraq, Using CA-Markov and ANN Models. *Sustainability* **2022**, *14*, 8568. [[CrossRef](#)]
23. Daba, M.H.; You, S. Quantitatively Assessing the Future Land-Use/Land-Cover Changes and Their Driving Factors in the Upper Stream of the Awash River Based on the CA-Markov Model and Their Implications for Water Resources Management. *Sustainability* **2022**, *14*, 1538. [[CrossRef](#)]
24. He, X.; Miao, Z.; Wang, Y.; Yang, L.; Zhang, Z. Response of Soil Erosion to Climate Change and Vegetation Restoration in the Ganjiang River Basin, China. *Ecol. Indic.* **2024**, *158*, 111429. [[CrossRef](#)]
25. Meng-Xia, Z.; Bu-Da, S.U.; Yan-Jun, W.; An-Qian, W.; Tong, J. Impacts of Climate Change on River Runoff at the Ganjiang and Guanting River Basins in the Eastern Monsoon Region. *Adv. Clim. Chang. Res.* **2020**, *16*, 679.
26. Zhang, Y.; Tang, C.; Ye, A.; Zheng, T.; Nie, X.; Tu, A.; Zhu, H.; Zhang, S. Impacts of Climate and Land-Use Change on Blue and Green Water: A Case Study of the Upper Ganjiang River Basin, China. *Water* **2020**, *12*, 2661. [[CrossRef](#)]
27. Huang, F.; Tao, S.; Li, D.; Lian, Z.; Catani, F.; Huang, J.; Li, K.; Zhang, C. Landslide Susceptibility Prediction Considering Neighborhood Characteristics of Landslide Spatial Datasets and Hydrological Slope Units Using Remote Sensing and GIS Technologies. *Remote Sens.* **2022**, *14*, 4436. [[CrossRef](#)]
28. Aalto, J.; Pirinen, P.; Heikkinen, J.; Venäläinen, A. Spatial Interpolation of Monthly Climate Data for Finland: Comparing the Performance of Kriging and Generalized Additive Models. *Theor. Appl. Climatol.* **2013**, *112*, 99–111. [[CrossRef](#)]
29. Ahmed, K.; Shahid, S.; Harun, S.B. Spatial Interpolation of Climatic Variables in a Predominantly Arid Region with Complex Topography. *Environ. Syst. Decis.* **2014**, *34*, 555–563. [[CrossRef](#)]
30. Amir Siddique, M.; Wang, Y.; Xu, N.; Ullah, N.; Zeng, P. The Spatiotemporal Implications of Urbanization for Urban Heat Islands in Beijing: A Predictive Approach Based on CA-Markov Modeling (2004–2050). *Remote Sens.* **2021**, *13*, 4697. [[CrossRef](#)]
31. Xu, D.; Zhang, K.; Cao, L.; Guan, X.; Zhang, H. Driving Forces and Prediction of Urban Land Use Change Based on the Geodetector and CA-Markov Model: A Case Study of Zhengzhou, China. *Int. J. Digit. Earth* **2022**, *15*, 2246–2267. [[CrossRef](#)]
32. Zimmermann, P.; Tasser, E.; Leitinger, G.; Tappeiner, U. Effects of Land-Use and Land-Cover Pattern on Landscape-Scale Biodiversity in the European Alps. *Agric. Ecosyst. Environ.* **2010**, *139*, 13–22. [[CrossRef](#)]
33. Gove, N.E.; Edwards, R.T.; Conquest, L.L. Effects of Scale on Land Use and Water Quality Relationships: A Longitudinal Basin-Wide Perspective. *JAWRA J. Am. Water Resour. Assoc.* **2001**, *37*, 1721–1734. [[CrossRef](#)]
34. Li, Q.; Zhang, H.; Guo, S.; Fu, K.; Liao, L.; Xu, Y.; Cheng, S. Groundwater Pollution Source Apportionment Using Principal Component Analysis in a Multiple Land-Use Area in Southwestern China. *Environ. Sci. Pollut. Res.* **2020**, *27*, 9000–9011. [[CrossRef](#)]
35. Jardim, A.M.d.R.F.; Júnior, G.D.N.A.; da Silva, M.V.; dos Santos, A.; da Silva, J.L.B.; Pandorfi, H.; de Oliveira-Júnior, J.F.; Teixeira, A.H.d.C.; Teodoro, P.E.; de Lima, J.L.M.P.; et al. Using Remote Sensing to Quantify the Joint Effects of Climate and Land Use/Land Cover Changes on the Caatinga Biome of Northeast Brazilian. *Remote Sens.* **2022**, *14*, 1911. [[CrossRef](#)]
36. Peng, X.; Wu, W.; Zheng, Y.; Sun, J.; Hu, T.; Wang, P. Correlation Analysis of Land Surface Temperature and Topographic Elements in Hangzhou, China. *Sci. Rep.* **2020**, *10*, 10451. [[CrossRef](#)]
37. Hu, S.; Fan, Y.; Zhang, T. Assessing the Effect of Land Use Change on Surface Runoff in a Rapidly Urbanized City: A Case Study of the Central Area of Beijing. *Land* **2020**, *9*, 17. [[CrossRef](#)]
38. Wang, Q.; Wang, H. An Integrated Approach of Logistic-MCE-CA-Markov to Predict the Land Use Structure and Their Micro-Spatial Characteristics Analysis in Wuhan Metropolitan Area, Central China. *Environ. Sci. Pollut. Res.* **2022**, *29*, 30030–30053. [[CrossRef](#)]
39. Hao, L.; He, S.; Zhou, J.; Zhao, Q.; Lu, X. Prediction of the Landscape Pattern of the Yancheng Coastal Wetland, China, Based on XGBoost and the MCE-CA-Markov Model. *Ecol. Indic.* **2022**, *145*, 109735. [[CrossRef](#)]
40. Wang, C.; Huang, S.; Wang, J. Spatio-Temporal Dynamic Evolution and Simulation of Dike-Pond Landscape and Ecosystem Service Value Based on MCE-CA-Markov: A Case Study of Shunde, Foshan. *Forests* **2022**, *13*, 1241. [[CrossRef](#)]
41. Yi, S.; Zhou, Y.; Li, Q. A New Perspective for Urban Development Boundary Delineation Based on the MCR Model and CA-Markov Model. *Land* **2022**, *11*, 401. [[CrossRef](#)]
42. Zhang, Z.; Hu, B.; Jiang, W.; Qiu, H. Identification and Scenario Prediction of Degree of Wetland Damage in Guangxi Based on the CA-Markov Model. *Ecol. Indic.* **2021**, *127*, 107764. [[CrossRef](#)]

43. Koko, A.F.; Yue, W.; Abubakar, G.A.; Hamed, R.; Alabsi, A.A.N. Monitoring and Predicting Spatio-Temporal Land Use/Land Cover Changes in Zaria City, Nigeria, through an Integrated Cellular Automata and Markov Chain Model (CA-Markov). *Sustainability* **2020**, *12*, 10452. [[CrossRef](#)]
44. Shi, P.; Zhang, Y.; Li, Z.; Li, P.; Xu, G. Influence of Land Use and Land Cover Patterns on Seasonal Water Quality at Multi-Spatial Scales. *CATENA* **2017**, *151*, 182–190. [[CrossRef](#)]
45. Faichia, C.; Tong, Z.; Zhang, J.; Liu, X.; Kazuva, E.; Ullah, K.; Al-Shaibah, B. Using RS Data-Based CA–Markov Model for Dynamic Simulation of Historical and Future LUCC in Vientiane, Laos. *Sustainability* **2020**, *12*, 8410. [[CrossRef](#)]
46. Abijith, D.; Saravanan, S. Assessment of Land Use and Land Cover Change Detection and Prediction Using Remote Sensing and CA Markov in the Northern Coastal Districts of Tamil Nadu, India. *Environ. Sci. Pollut. Res.* **2022**, *29*, 86055–86067. [[CrossRef](#)]
47. Tadese, S.; Soromessa, T.; Bekele, T. Analysis of the Current and Future Prediction of Land Use/Land Cover Change Using Remote Sensing and the CA-Markov Model in Majang Forest Biosphere Reserves of Gambella, Southwestern Ethiopia. *Sci. World J.* **2021**, *2021*, e6685045. [[CrossRef](#)] [[PubMed](#)]
48. Huang, Y.; Xie, F.; Song, Z.; Zhu, S. Evolution and Multi-Scenario Prediction of Land Use and Carbon Storage in Jiangxi Province. *Forests* **2023**, *14*, 1933. [[CrossRef](#)]
49. Hua, F.; Bruijnzeel, L.A.; Meli, P.; Martin, P.A.; Zhang, J.; Nakagawa, S.; Miao, X.; Wang, W.; McEvoy, C.; Peña-Arancibia, J.L.; et al. The Biodiversity and Ecosystem Service Contributions and Trade-Offs of Forest Restoration Approaches. *Science* **2022**, *376*, 839–844. [[CrossRef](#)]
50. Ahammad, R.; Stacey, N.; Sunderland, T.C.H. Use and Perceived Importance of Forest Ecosystem Services in Rural Livelihoods of Chittagong Hill Tracts, Bangladesh. *Ecosyst. Serv.* **2019**, *35*, 87–98. [[CrossRef](#)]
51. Lai, Z.; Chen, M.; Liu, T. Changes in and Prospects for Cultivated Land Use since the Reform and Opening up in China. *Land Use Policy* **2020**, *97*, 104781. [[CrossRef](#)]
52. Zhang, Q.; Ye, H.; Ding, Y.; Cao, Q.; Zhang, Y.; Huang, K. Carbon Storage Dynamics of Subtropical Forests Estimated with Multi-Period Forest Inventories at a Regional Scale: The Case of Jiangxi Forests. *J. For. Res.* **2020**, *31*, 1247–1254. [[CrossRef](#)]
53. Liang, Y.; Hashimoto, S.; Liu, L. Integrated Assessment of Land-Use/Land-Cover Dynamics on Carbon Storage Services in the Loess Plateau of China from 1995 to 2050. *Ecol. Indic.* **2021**, *120*, 106939. [[CrossRef](#)]
54. Sha, Z.; Bai, Y.; Li, R.; Lan, H.; Zhang, X.; Li, J.; Liu, X.; Chang, S.; Xie, Y. The Global Carbon Sink Potential of Terrestrial Vegetation Can Be Increased Substantially by Optimal Land Management. *Commun. Earth Environ.* **2022**, *3*, 1–10. [[CrossRef](#)]
55. Zhang, X.; Xie, H.; Shi, J.; Lv, T.; Zhou, C.; Liu, W. Assessing Changes in Ecosystem Service Values in Response to Land Cover Dynamics in Jiangxi Province, China. *Int. J. Environ. Res. Public Health* **2020**, *17*, 3018. [[CrossRef](#)] [[PubMed](#)]
56. Chazdon, R.L.; Falk, D.A.; Banin, L.F.; Wagner, M.; Wilson, S.J.; Grabowski, R.C.; Suding, K.N. The Intervention Continuum in Restoration Ecology: Rethinking the Active–Passive Dichotomy. *Restor. Ecol.* **2021**, e13535. [[CrossRef](#)]
57. Kanowski, J.; Catterall, C.P. Carbon Stocks in Above-Ground Biomass of Monoculture Plantations, Mixed Species Plantations and Environmental Restoration Plantings in North-East Australia. *Ecol. Manag. Restor.* **2010**, *11*, 119–126. [[CrossRef](#)]
58. Chazdon, R.L.; Uriarte, M. Natural Regeneration in the Context of Large-Scale Forest and Landscape Restoration in the Tropics. *Biotropica* **2016**, *48*, 709–715. [[CrossRef](#)]
59. Naime, J.; Mora, F.; Sánchez-Martínez, M.; Arreola, F.; Balvanera, P. Economic Valuation of Ecosystem Services from Secondary Tropical Forests: Trade-Offs and Implications for Policy Making. *For. Ecol. Manag.* **2020**, *473*, 118294. [[CrossRef](#)]
60. Brancalion, P.H.S.; Amazonas, N.T.; Chazdon, R.L.; van Melis, J.; Rodrigues, R.R.; Silva, C.C.; Sorrini, T.B.; Holl, K.D. Exotic Eucalypts: From Demonized Trees to Allies of Tropical Forest Restoration? *J. Appl. Ecol.* **2020**, *57*, 55–66. [[CrossRef](#)]
61. Betts, M.G.; Phalan, B.T.; Wolf, C.; Baker, S.C.; Messier, C.; Puettmann, K.J.; Green, R.; Harris, S.H.; Edwards, D.P.; Lindenmayer, D.B.; et al. Producing Wood at Least Cost to Biodiversity: Integrating Triad and Sharing–Sparing Approaches to Inform Forest Landscape Management. *Biol. Rev.* **2021**, *96*, 1301–1317. [[CrossRef](#)] [[PubMed](#)]
62. Strassburg, B.B.N.; Iribarrem, A.; Beyer, H.L.; Cordeiro, C.L.; Crouzeilles, R.; Jakovac, C.C.; Braga Junqueira, A.; Lacerda, E.; Latawiec, A.E.; Balmford, A.; et al. Global Priority Areas for Ecosystem Restoration. *Nature* **2020**, *586*, 724–729. [[CrossRef](#)]
63. Brancalion, P.H.S.; Niamir, A.; Broadbent, E.; Crouzeilles, R.; Barros, F.S.M.; Almeyda Zambrano, A.M.; Baccini, A.; Aronson, J.; Goetz, S.; Reid, J.L.; et al. Global Restoration Opportunities in Tropical Rainforest Landscapes. *Sci. Adv.* **2019**, *5*, eaav3223. [[CrossRef](#)]
64. Tatum, M. China’s Three-Child Policy. *Lancet* **2021**, *397*, 2238. [[CrossRef](#)] [[PubMed](#)]
65. Deng, T.; Wang, D.; Yang, Y.; Yang, H. Shrinking Cities in Growing China: Did High Speed Rail Further Aggravate Urban Shrinkage? *Cities* **2019**, *86*, 210–219. [[CrossRef](#)]

**Disclaimer/Publisher’s Note:** The statements, opinions and data contained in all publications are solely those of the individual author(s) and contributor(s) and not of MDPI and/or the editor(s). MDPI and/or the editor(s) disclaim responsibility for any injury to people or property resulting from any ideas, methods, instructions or products referred to in the content.